

HETEROCYCLES, Vol. 102, No. 4, 2021, pp. 622 - 646. © 2021 The Japan Institute of Heterocyclic Chemistry
Received, 14th August, 2020, Accepted, 30th September, 2020, Published online, 20th October, 2020
DOI: 10.3987/REV-20-942

MINI REVIEW: ANTIOXIDANT APPLICATION OF METAL-ORGANIC FRAMEWORKS AND THEIR COMPOSITES

Shaikha S. Alneyadi^{1*}

¹Department of Chemistry, College of Science, UAE University Al-Ain, 15551
UAE

Abstract – Metal–organic frameworks (MOFs) are porous coordination materials composed of multidentate organic ligands and metal ions or metal clusters. MOFs have great potential as medical materials for biological, environmental, and food antimicrobial fields. In recent years, MOFs have been applied to various antioxidant fields due to their continued release capability, porosity, and structural flexibility in combination with many chemicals and/or materials such as nanoparticles, antioxidant, and polymers. This review offers a detailed summary of the antioxidant applications of MOFs and their composites, focusing on the combination types of MOF composites and their antioxidant effects in different applications described in 2015-2020. These applications are illustrated by the examples discussed in this review.

CONTENTS

1. Introduction
 - 1.1 Antioxidants as a ligand in the MOF structure
 - 1.1.1 Mg(H₂gal) system
 - 1.1.2 MIL-155 and MIL-156 systems
 - 1.2 Antioxidant Encapsulated in MOFs
 - 1.2.1 SC@FNPCN-333 system
 - 1.2.2 CD-MOF/curcumin system
 - 1.2.3 CD-MOF/catechins system
 - 1.2.4 CD-MOF/chitosan-resveratrol system
 - 1.2.5 FER@MFM-300(Sc) system
 - 1.2.6 Quercetin@ZIF-90 system
2. Conclusions

1. INTRODUCTION

Antioxidants are molecules that can safely interact with free radicals, terminate the chain reaction, and convert them to a harmless molecules through the donation of an electron or proton to scavenge reactive oxygen species.¹ In the current decade, antioxidants have drawn attention due to their potential to minimize oxidative stress, which is defined as the pathophysiological response created via the imbalance between the production of oxidants and the endogenous antioxidants that counteract the effects of the oxidants. There is a net increase in reactive oxygen species (ROS) such as superoxide anions, hydroxyl radicals (HO•), hydrogen peroxide (H₂O₂), singlet oxygen (¹O₂), and reactive nitrogen species (RNS; e.g., peroxynitrite).² ROS and RNS are generally induced by endogenous routes including ROS generating enzymes (e.g., nitric oxide synthase, xanthine oxidase) and cellular metabolic functions (e.g., secretion by macrophages, electron transport chain by-products), as well as by external sources like environmental stress (e.g., ionizing radiation, redox, and heavy metals, excess UV-radiation). ROS and RNS can react with and cause damage to cell membranes, membranes of subcellular organelles, proteins, lipids, and DNA, which all impair the normal functioning of the cells and can lead to mutations, apoptosis, and system failure.³ Thus, at a systematic level, oxidative stress plays a role in the development and acceleration of many diseases including diabetes, cardiovascular diseases, Alzheimer's and Parkinson's disease, acute renal failure, acute lung injury, radiation injury, cancer, arthritis, and aging.⁴ Almost all organisms have built-in endogenous antioxidant defense and repair systems to protect against oxidative damage, which very frequently are inadequate to completely prevent the damage.⁵ Therefore, the use of antioxidant supplements is recommended to reduce oxidative damage to the human body.

Antioxidants generally exert their activity by two main mechanisms, either by preventing the formation of ROS/RNS or scavenging/neutralizing ROS/RNS. In some cases, antioxidants, specifically enzymatic compounds, decompose ROS/RNS into less harmful or neutral products.⁶ Many different chemical compounds have been evaluated for their antioxidant properties. These compounds may be either endogenous (e.g., glutathione and uric acid) or exogenous based on their origin, but the majority of antioxidants come from diet.⁷ They may be naturally derived, synthetic, or in organic materials at the nanoscale level, or the most interesting and recently explored, nano-encapsulated antioxidant molecules. Natural antioxidants have the ability to potentially modulate oxidative stress. Several fruits, vegetables, and fruit by-products have been screened for antioxidant compounds such as vitamins (ascorbic acid), carotenoids (lutein), polyphenols (3,6-dihydroxyflavone), and metabolic sensitizers (methyl selenocysteine), which scavenge excess free radicals from the human body.⁸ Moreover, antioxidants derived from natural resources such as gallic acid (GA) and dried rose flower extracts like *Rosa rugosa*, as well as bioactive compounds derived from different sources, have also exhibited potential antioxidant capacity, the ability to scavenge active oxygen species and electrophiles, inhibit nitrosation reactions, and

act in the decrement of lipid peroxidation level.⁹ However, natural antioxidants are prone to degradation and their bioavailability is limited by low absorption and degradation during delivery.¹⁰

Some synthetic compounds, such as butylated hydroxyanisole (BHA) and butylated hydroxytoluene (BHT), BHT analogs, and GA esters have been used as antioxidants⁸ and have shown to have negative health influences; hence, their applications have been restricted and replaced by naturally occurring dietary antioxidants.¹¹ However, the development of nanotechnology has discovered numerous nanoparticles either from inorganic¹² or biological origins, as potent antioxidants. Novel metal nanoparticles (Au, Ag, Pt) and transition metal oxides (CuO, NiO) are normally used for their antioxidant activity.¹² Moreover, nanocomposites either in single or bi-metallic combination, prepared by chemical or green techniques from phytochemicals (leaf extracts), were also assessed for antioxidant activity.¹³ However, the antioxidant activity of these nanoparticles depends on their nature, chemical composition, surface charge, particle size, surface to volume ratio, and surface coating.¹⁴ Nanoparticles offer several advantages over traditional antioxidant delivery methods, including environmental protection of bioactive components, increased bioavailability, targeted delivery of antioxidants, and controlled release at the site of action. However, achieving high specificity against ROS is the main difficulty to these antioxidants, which may cause them to fail to prevent oxidative damage completely. In addition, oxidative stress, immune cell activation, mitochondrial respiration, and genotoxicity are the major challenges for *in vivo* applications of these exogenous nanomaterials that may also contribute to potential deleterious health effects.¹⁵ Diverse approaches have been established to overcome limitations of traditional pharmacological treatments (e.g., biodegradation, low specificity, toxicity, side effects). Remarkably, the use of nanoplateforms like Drug Delivery Systems can be used to control the dose and delivery kinetics of active drugs, suggesting they are a promising new generation of modified treatments. MOFs presented a suitable alternative to other mesoporous materials such as zeolites and mesoporous silica particles and in some cases, exhibited higher drug loading and more controlled deliveries.

MOFs generally refer to porous materials in which organic ligands and metal ions form a network structure through self-assembly.¹⁶ Metal ions or metal ion clusters and organic molecules called a linker building are the two main components of MOFs, which could create an unlimited network structure through the coordination or covalent bond connections of the metal ion center and organic ligands.¹⁷ The metal ions and ligands have a richness of geometry and connectivity and consequently, the physicochemical properties of MOFs can be artificially designed for and adjusted to various applications.¹⁸ They have the advantages of high specific surface area, adjustable pore structure, and controlled ion release rate compared with the traditional antioxidant materials.

MOFs can be prepared to have high porosity as well as contain a variety of pore shapes. By selecting the appropriate structure and shape of the organic ligands, the composition and size of MOF pores can be

controlled, thereby defining the porosity and specific surface area of the skeleton. This can lead to the design of a final porous material that is suitable for different requirements.¹⁹ In the early stages of MOF development, most of their applications were in catalysis, separation, and storage of gas mixtures.¹⁸ However, the applications of MOFs are now expanding to include energy storage devices, sensors detection, hazardous material adsorption, new catalysis, and biomedical applications.²⁰ The MOF preparation methods have continuously evolved due to their extensive application potential. Today, various methods for preparing MOFs have been reported, including common solvothermal/hydrothermal synthesis, sonochemical synthesis, microwave-assisted synthesis, electrochemical synthesis, mechanochemical synthesis, ionothermal processes, and microfluidic synthesis or dry gel conversion.²¹ Because of the diversity in the synthesis methods and their resulting available structures, MOFs and their composites offer a range of options to develop novel antioxidant materials that can substitute for traditional ones. MOFs can be used as a reservoir for antioxidant agents due to their composition, construction, and internal extensive surface volume, which are all aspects of the advantage of MOFs as a new high-performance antioxidant material. In addition, MOFs can encapsulate antioxidant substances during their construction, and the benefit of MOFs over natural or synthetic materials containing metal ions is the uniform distribution of the metal active sites. Furthermore, the organic ligands used to synthesize MOFs themselves may also have antioxidant activity. Ligand molecules can be stored in the spatial structure inside the MOFs so that the metal ions and the antioxidant properties of the organic ligand can be combined to produce a synergistic effect.

Here, we review how MOFs can be combined with different materials, including slow-release antioxidant delivery, antioxidant coatings with high polymer materials, and high-efficiency antioxidant materials combined with nanoparticles (NPs). We aimed to summarize the antioxidant applications of MOFs and their composites (Table 1). All aspects concerning various antioxidant applications, including MOFs as the reservoir to release drug in sterilization, and MOFs combined with other materials to form antioxidant composites, as well as the prospects for improved antioxidant strategies in biological, environmental, and food antioxidant fields will be discussed. Hence, in this review, antioxidant applications were categorized based on antioxidant incorporation and delivery from biocompatible metal–organic frameworks into (1) antioxidants as organic linkers in MOF structures or (2) antioxidants encapsulated within the pores of the MOF. Detailed discussion of MOF properties, stability, potency, and most importantly, delivery strategies and antioxidant are also outlined.

1.1 ANTIOXIDANTS AS A LIGAND IN THE MOF STRUCTURE

1.1.1 Mg(H₂gal) SYSTEM

Cooper *et al.*²² reported the synthesis of a new porous magnesium gallate based MOF (Mg(H₂gal)·2H₂O) prepared from biocompatible reagents and *in vitro* evaluated for antioxidant activity through the progressive delivery of its active organic linker upon MOF degradation. Mg(H₂gal)·2H₂O is prepared from a biofriendly cation (Mg²⁺) and organic ligand (gallic acid, H₄gal). The antioxidant activity of gallic acid (H₄gal) has been studied and is related to several useful therapeutic effects, including anti-allergic, anti-inflammatory, antimicrobial, cardioprotective, neuroprotective and even, anticarcinogenic activities.²³ Mg(II) metal has been used in the formation of many MOFs of interest²⁴ and is involved in oxidative stress resistance, suggesting it could have additional benefits when coupled with antioxidative species.²⁵ In a study that focused on the combinations combination of the natural ligand (H₄gal) and nontoxic metal Mg(II),²⁶ the Mg(H₂gal)·2H₂O was prepared by mixing 10 g MgCl₂, 38 g H₄gal, and water. The reaction mixture was stirred under reflux and then adjusted to pH 8 with 10 M potassium hydroxide before the mixture was heated at 120 °C for 24 h. The light grey solid product was collected by filtration, washed with water, and air-dried to obtain the Mg(H₂gal) with a 77% yield (Figure 1). The structure of the Mg(H₂gal)·2H₂O consists of chains of corner sharing MgO₆ distorted octahedra (four oxygen atoms coming from the phenol groups and two from the carboxyl functions) connected through the organic ligands which define small channels containing water molecules.²²

MOFs were first considered for controlled drug release through physisorption/desorption processes,²⁷ however, the incorporation of an active molecule within the framework that could be released by the degradation of the framework itself was recently proposed as a promising alternative.²⁸ In comparison with the traditional sorption-based method, this approach allows for the release of a larger amount of active molecule with a release kinetics that is dependent on the degradation rate, which avoids the use of exogenous compounds with unknown toxicity. The degradation profiles of Mg(H₂gal)·2H₂O show that the gallic acid is released slowly into the solution (45% after 1 day), confirming that Mg(H₂gal)·2H₂O acts as a controlled release source of gallic acid with very limited cytotoxicity detected. The antioxidant properties of Mg(H₂gal)·2H₂O were evaluated in the HL-60 cell line by the production of reactive oxygen species (ROS). Concentrations of 60 μg mL⁻¹ Mg(H₂gal)·2H₂O significantly reduced ROS production by phorbol 12-myristate-13-acetate (PMA), confirming the effective antioxidant activity of Mg(H₂gal)·2H₂O. In addition, because of its porosity (SBET ~ 330 m²g⁻¹, calculated pore volume ~0.16 cm³/g), Mg(H₂gal)·2H₂O could trap and release small bio-gases (e.g., NO, CO) and hence, could be used to achieve combined bio-activities in the near future.²⁹

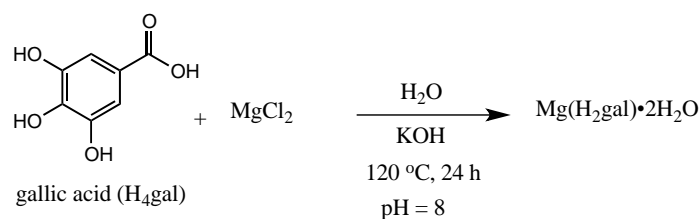


Figure 1. Synthesis of $\text{Mg}(\text{H}_2\text{gal}) \cdot 2\text{H}_2\text{O}$

1.1.2 MIL-155 AND MIL-156 SYSTEMS

Hidalgo *et al.*³⁰ extended their study by determining the activity of gallic acid with another nontoxic metal (calcium), in order to evaluate the impact of the composition and structure on the antioxidant of these materials. Two novel 3-D coordination polymers, MIL-155 and MIL-156, were hydrothermally synthesized from calcium and naturally occurring gallic acid (H_4gal). These solids are based on different inorganic subunits: infinite chains of edge-sharing dimers of CaO_7 polyhedra linked through partially deprotonated gallate ligands ($\text{H}_2\text{gal}^{2-}$) for MIL-155 ($[\text{Ca}_2(\text{H}_2\text{O})(\text{H}_2\text{gal})_2] \cdot 2\text{H}_2\text{O}$), and ribbon-like inorganic subunits containing both eight-fold or six-fold coordinated $\text{Ca}(\text{II})$ ions linked through fully deprotonated gallate ligands (gal^{4-}) for MIL-156 or ($[\text{Ca}_3\text{K}_2(\text{H}_2\text{O})_2(\text{gal})_2] \cdot n\text{H}_2\text{O}$ ($n \sim 5$)). Both solids contain small channels filled with water molecules that do not have accessible porosity towards N_2 at 77 K.

The MIL-155 was prepared by dissolving 2 mM gallic acid monohydrate in 10 mL distilled water at room temperature. Then, 1 mM calcium nitrate was added and adjusted to pH 8 with 5M potassium hydroxide solution. The reaction mixture was then heated to 120 °C for 12 h (Figure 2). MIL-156 was synthesized by mixing an aqueous solution of 1 mM gallic acid monohydrate with 1 mM calcium hydroxide and adjusted to pH 14 with 5 M potassium hydroxide. The reaction mixture was then heated up to 120 °C for 24 h (Figure 3).

Both MIL-155 and MIL-156 have suitable biocompatibility, evidenced by the high cell viability and low presence of apoptotic cells when several cell lines were incubated with the solids. Although made of the same constituents, these solids exhibit different composition and crystal structures that lead to very different solubility in simulated biological media and therefore, present different antioxidant activities. While MIL-156 does not show any antioxidant effect because of its high chemical stability, the progressive release of the gallate ligand from the less stable MIL-155 has a remarkable protective antioxidant effect that is concentration-dependent. Comparing these results with the previously reported for $\text{Mg}(\text{H}_2\text{gal})$,²² we notice a higher efficacy for MIL-155. Indeed, while only the highest tested doses of $\text{Mg}(\text{H}_2\text{gal})$ (60 mg mL^{-1}) show antioxidant activity, MIL-155 has a protective activity at much lower concentrations, starting from 5 mg mL^{-1} . The concentration of released gallate in solution was very

similar in the media for both solids (0.17 vs. 0.19 mg mL⁻¹ for MIL-155 and Mg(H₂gal), respectively), suggesting the cation can influence the oxidant effect.

In contrast to magnesium, calcium is known to be indirectly involved in ROS balance. Indeed, high intracellular calcium levels can induce ROS production, which is related with the disruption of the mitochondrial membrane, and consequently, cell apoptosis.³¹ However, this seems to conflict with the findings of Hidalgo *et al.*,³⁰ that showed a lower ROS. Although more specific studies are needed to elucidate the antioxidant mechanism, one hypothesis is that the presence of the gallate linker can modify the intracellular calcium levels (i.e., by coordination). Hence, antioxidant based MOFs appear to be promising candidates not only for bio-applications (e.g., dermatology, wound healing,³² skin-whitening cosmetics by melanogenesis inhibition),³³ but also for food preservation (e.g., antimicrobial activity,³⁴ lipid oxidation prevention),³⁵ smart surfaces,³⁶ and cancer therapy (e.g., inhibition of carcinogenesis,³⁷ prevention of lung cancer).³⁸

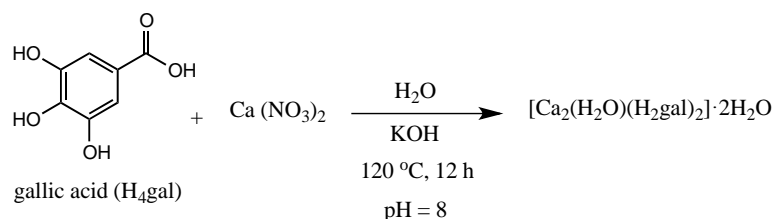


Figure 2. Synthesis of MIL-155

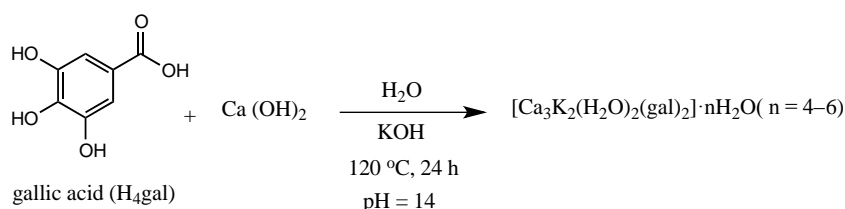


Figure 3. Synthesis of MIL-156

1.2 ANTIOXIDANT ENCAPSULATED IN MOFS

1.2.1 SC@FNPCN-333 SYSTEM

Improving enzymatic function in cells is needed for applications ranging from *ex vivo* cellular manipulations to enzyme replacement therapies in humans. However, because enzymes degrade in biological milieus, achieving long-term enzymatic activity can be challenging. Recently, enzymes have been loaded into the MOF cavities and immobilized enzymes tested thus far (e.g., horseradish peroxidase (HRP), and cytochrome c (Cyt c)) have displayed robust *in vitro* activities.³⁹ These results indicate that proteins can fold properly in the cavities of MOFs and remain functionally active. MOF-immobilized

enzymes have also shown unexpected stabilities under denaturing conditions such as extreme heat, high or low pH, and in the presence of organic solvents.⁴⁰ Moreover, the cage formed by MOFs around the enzyme acts as a barrier against proteases, such as trypsin, and protects the encapsulated proteins from proteolytic degradation.⁴¹

Lian *et al.*⁴² reported a new system that consists of antioxidative enzymes encapsulated in metal–organic frameworks. They demonstrated that, while free enzymes had weak activity for only a short duration of time, this system could protect human cells from toxic reactive oxygen species for up to a week, regardless of the system being localized in lysosomes, which are acidic organelles that contain a variety of proteases. The long-term persistence of the system was due to the chemical stability of MOF in low pH environments and to the protease resistance provided by the protective cage formed by the MOF around the encapsulated enzymes. The authors concluded that intracellular MOF system was capable of supporting a sustained and beneficial enzymatic activity to living cells. They selected NPCN-333(Al) as a MOF platform due to its high enzyme encapsulation capacity, facile fluorescence alteration, and good chemical robustness in aqueous solutions.⁴³ The NPCN-333(Al) can contain antioxidant enzymes, superoxide dismutase (SOD), and catalase (CAT), which protected cells from severe oxidative stress.⁴⁴

The PCN-333(Al) was prepared by mixing $\text{AlCl}_3 \cdot 6\text{H}_2\text{O}$ with 4,4',4''-s-triazine-2,4,6-triyl-tribenzoic acid (TATB) in DMF and heating the mixture at 95 °C for 24 h (Figure 4). The surface area was $2793 \text{ m}^2\text{g}^{-1}$ and the void volume was $2.94 \text{ cm}^3\text{g}^{-1}$ for the MOP platform. FNPCN333 is a fluorescent version of NPCN-333 that was prepared via ligand metathesis of NPCN-333 with a BTB ligand functionalized with the BODIPY fluorophore. FNPCN-333 was synthesized by dispersing the NPCN-333 in DMF, to which a solution of BTB Green was added. The mixture was incubated in an 85 °C oven for 4 h (Figure 5). The ligand ratio of BTB Green/TATB was 1:6. FNPCN-333 displayed a particle size, distribution, and porosity properties that were similar to those of NPCN-333 (surface area $2428 \text{ m}^2\text{g}^{-1}$, void volume $2.30 \text{ cm}^3\text{g}^{-1}$). However, unlike NPCN-333, FNPCN-333 was fluorescent with a maximal emission at 509 nm in water.

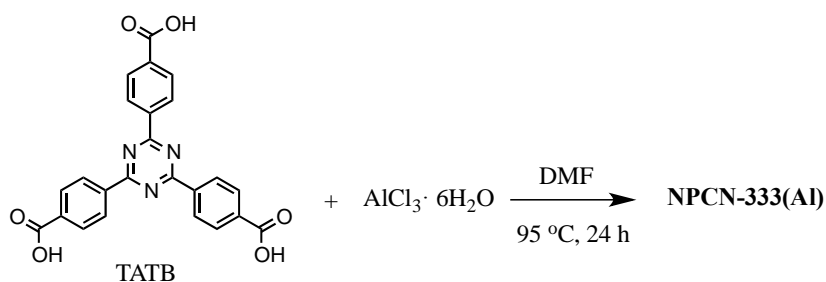


Figure 4. Synthesis of NPCN-333(Al)

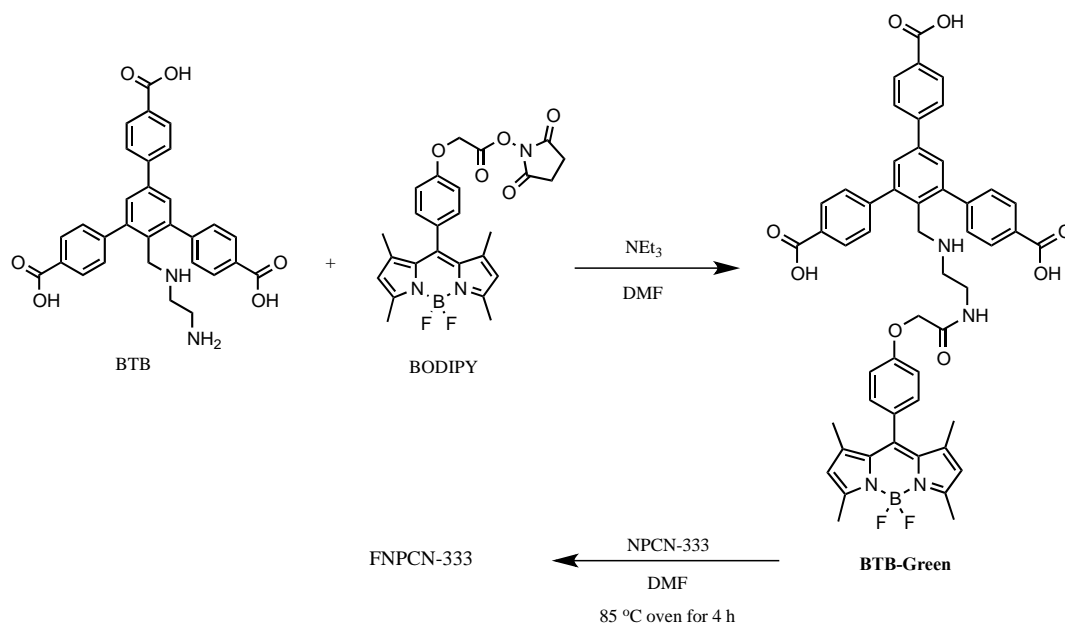


Figure 5. Synthesis of FNPCN-333

The molecular dimensions of SOD ($2.8 \times 3.5 \times 4.2 \text{ nm}^3$, 16.3 kDa)⁴⁵ and CAT ($4.9 \times 4.4 \times 5.6 \text{ nm}^3$, 60 kDa)⁴⁶ indicated that they could theoretically fit into the 4.0 nm and 5.5 nm cavities of FNPCN-333, respectively. Two enzymes were incorporated into FNPCN-333 in a stepwise fashion. First, FNPCN-333 was incubated with CAT so it could occupy the larger MOF cavities, and then, FNPCN-333 was incubated with SOD to load the smaller cavities that would not accommodate CAT. Based on BCA analysis, the encapsulation capacity of FNPCN-333 for SOD and CAT was 0.80 gg^{-1} and 1.26 gg^{-1} , respectively, which was equivalent to the calculated values of the highest encapsulation capacity (0.92 gg^{-1} and 1.74 gg^{-1}) and indicated a high loading efficiency.

The antioxidant activity results confirmed that SC@FNPCN-333 can protect cells from ROS-induced toxicity by eliminating ROS species. It is noteworthy that the proximity of SOD and CAT in the enzymatic nanofactory improved the protective effect against paraquat (PQ)-induced oxidative stress. SOD catalyzes the disproportionation of superoxide and generates H_2O_2 and oxygen, while H_2O_2 is consumed by CAT to produce water and oxygen. Since the two reactions catalyzed by SOD and CAT may happen in a cascade manner, it is likely that SOD-generated H_2O_2 is degraded by CAT before the ROS diffuses away from the nanofactory. This protective effect was reported for a minimum of one week even with the localization of the MOFs inside lysosomes.⁴⁷ Although the cytotoxicity of SC@FNPCN-333 was negligible, if MOF nanoparticles carried only SOD, the H_2O_2 generated by S@FNPCN-333 may diffuse away from C@FNPCN-333 before detoxification. The ROS that escapes the nanofactories may reach the cytosol and cause oxidative damage that could induce toxicity.

This study⁴² establishes that enzymatic nanofactories based on MOF can sustain intracellular enzymatic

activities for a long period of time. The proteins encapsulated within the MOF structure are enzymatically active, indicating that enzymes are properly folded and maintained within the MOF and that soluble substrates and products can diffuse in and out of the MOF-enzyme nanofactories. The MOF environment may stabilize the folding/structure of encapsulated enzymes, which would also contribute to improved protease resistance and could explain how the MOF prevents pH-induced unfolding and loss of enzymatic activity. For example, the diameter of the MOF cavities is tunable, which provides encapsulation of differently sized enzymes. It is also possible to encapsulate an enzyme cocktail that can have synergistic effects on biological systems, as confirmed by the results presented for SC@FNPCN-333. MOF-encapsulated enzymes remain accessible to substrates without the need of enzyme release from the carrier; indeed, the activity of encapsulated enzymes is comparable to that of the enzymes in their free form. The MOF encapsulation protects enzymes from proteolytic degradation and therefore, does not compromise enzymatic activity and in turn, allows for simple design and nanoparticle synthesis without need for release strategies.

1.2.2 CD-MOF/CURCUMIN SYSTEM

Based on its beneficial biological and pharmacological activities, curcumin has been found to have various important biological applications as an anti-inflammatory molecule,⁴⁸ along with its antioxidant activity⁴⁹ and ability to affect major cell signaling pathways. Curcumin is known to be unstable in neutral and alkaline conditions, undergoing hydrolytic degradation to feruloyl methane, ferulic acid, and vanillin.⁵⁰ Therefore, the exposure of curcumin to alkaline foods or components may be hard to avoid and thus, it should be protected from physical and chemical damage before its industrial use.

Several approaches have been tried to improve the delivery of curcumin in its intact hydrophobic form. Moussa *et al.*⁵¹ reported successful encapsulation of curcumin in cyclodextrin-metal-organic framework (CD-MOF), while Smaldone *et al.*⁵² synthesized CD-MOFs by mixing 1.0 molar-equivalent of cyclodextrin (1.30 g) with 8.0 molar-equivalents of potassium hydroxide (0.45 g) in 20 mL deionized distilled water while stirring for 6–12 h. The ratio of metal salt (KOH) to γ -CD was 1:8. The solution was filtered and sealed in a beaker containing 50 mL methanol to allow for vapor diffusion for 7 d at 23 ± 0.1 °C, after which a yield of approximately 85% CD-MOF crystals was obtained. To study the inclusion of curcumin, 10 mg CD-MOF crystals were dispersed in 3 mL methanol. Curcumin was dissolved in methanol and added to obtain a 25 μ M final concentration (Figure 6). The encapsulation kinetics were relatively slow with a half-life of 5.41 h under the experimental conditions. The results established that curcumin sat in the pores of CD-MOFs through a hydrogen bond interaction between the OH-group of the cyclodextrin moiety of the CD-MOFs and the phenolic hydroxyl group of curcumin. Moreover, the presence of curcumin did not disturb the CD-MOF crystallinity. The solvent polarity of the pores inside

the CD-MOFs was methanolic; therefore, dissociation of the curcumin-loaded CD-MOF in water did not separate curcumin from the dissolved framework, but resulted in the formation of an adduct in which a unique interaction occurred through the complexation of potassium ions with curcumin and CD. The dissociated framework loaded with curcumin molecules illustrated an important enhancement in the chemical stability of curcumin in aqueous alkaline conditions. In conclusion, CD-MOFs are a promising benign system in which to store and stabilize curcumin for food applications.

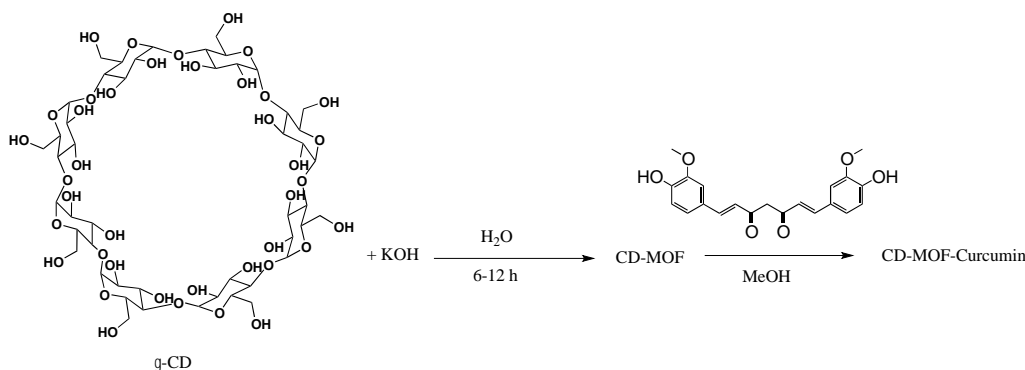


Figure 6. Schematic representation of synthesis of CD-MOF for curcumin loading

1.2.3 CD-MOF/CATECHINS SYSTEM

Green tea catechins have received significant attention due to their potent antioxidant activity and diverse biological properties. Stabilizing and protecting catechins from degradation are very important but challenging, and γ -cyclodextrin-based MOFs (CD-MOFs) have great potential to overcome this problem. CD-MOFs can be easily built from precursors γ -cyclodextrin (γ -CD) and alkali metal salts.⁵³ They have body-centered cubic structures and large spherical pores 1.7 nm in diameter, that are accessible through small 0.78-nm windows.⁵⁴ Zhou *et al.*⁵⁵ reported a promising catechin encapsulation system based on nanoscale CD-MOF for antioxidant activity in *in vitro*. The nontoxic and biocompatible CD-MOF nanocarriers can be prepared using a simple modified vapor diffusion method (Figure 7).

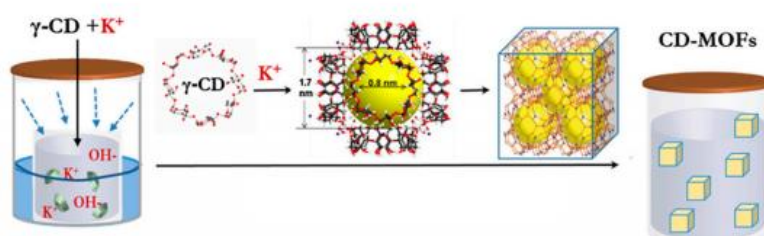


Figure 7. Vapor diffusion method⁸⁷

The CD-MOF was prepared by mixing 0.324 g γ -CD and 0.112 g KOH in deionized water at room temperature. Then, 5 mL ethanol was added as an emulsifier. The solution was sealed in a beaker

containing 5 mL methanol to allow for vapor diffusion in the aqueous solution at 50 °C. After 6 h incubation, the supernatant was transferred into a clean glass tube and another 10 mL methanol was added dropwise into the obtained suspension. The mixture was incubated at room temperature for 1 h and the products were collected by centrifugation, washed with methanol, and dried under vacuum for 12 h at 45 °C. Then, 50 mg epigallocatechin gallate (EGCG) dissolved in 10 mL ethanol, and the dehydrated CD-MOF (100 mg) were added. This mixture was stirred for 36 h at room temperature before the EGCG-loaded CD-MOF were collected by filtration and washed rapidly with 5 mL ethanol to remove the EGCG on the outer surface of the CD-MOFs. The sample was dried at the room temperature (Figure 8). The Brunauer–Emmett–Teller (BET) surface area and pore volume of the CD-MOFs were calculated to be 175 m²g⁻¹ and 0.11 cm³g⁻¹, respectively. After the catechin encapsulation, the BET surface area and pore volume of the nanocrystals decreased to 45 cm²g⁻¹ and 0.03 cm³g⁻¹, respectively, implying that the EGCG occupied almost the entire pore space in the frameworks.⁵⁵

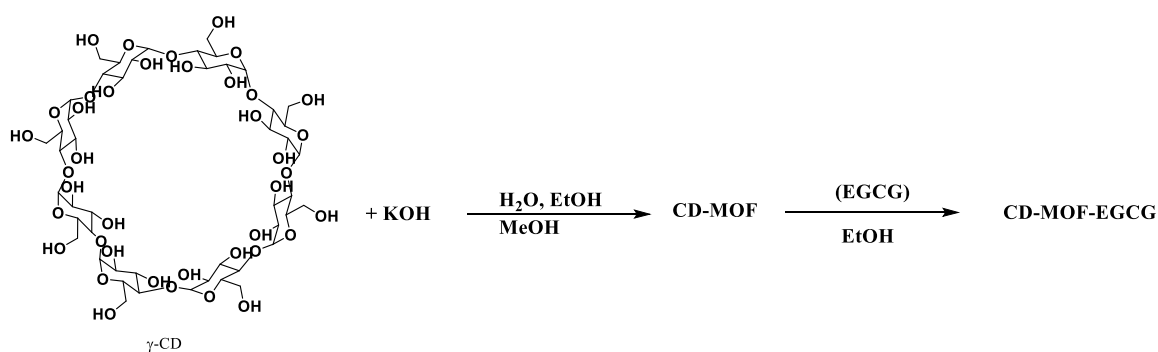


Figure 8. Schematic representation of synthesis of CD-MOF for EGCG loading

Antioxidant activity of the samples was evaluated and the efficiency of the free and encapsulated EGCG at different doses were compared. The antioxidant activity of CD-MOF-EGCG showed significant chemical stability of the EGCG in alkaline solutions; the amount of CD-MOF-EGCG increased from 1 mg to 4 mg, and the antioxidant activity gradually increased from 12% to 50%. When the cytotoxicity was analyzed, the authors found that the CD-MOF nanocrystals were safe and nontoxic. These findings demonstrate the significant potential of scaled-up synthesis of nanoscale CDMOF and the exploration of their ability to store and stabilize catechins for biomedical applications.

1.2.4 CD-MOF/CHITOSAN-RESVERATROL SYSTEM

Qiu *et al.*⁵⁶ reported a new nanocapsules system with a cyclodextrin metal-organic framework/chitosan (CD-MOF/CS) that has a hydrophobic core and hydrophilic shell that was prepared as a delivery system for bioactive agents. The nanocapsules were prepared using an electrostatic deposition approach to place

cationic chitosan onto the anionic CD-MOF core. Chitosan (CS) is the only cationic polysaccharide in nature; therefore, coating nanoparticles with chitosan, particularly edible organic nanoparticles, has received attention for their less toxic, good biocompatibility, and diverse applications.⁵⁷

Resveratrol, a triphenolic phytoalexin, is also naturally produced by various plant species such as grapes, mulberries, and pistachio.⁵⁸ Recently, resveratrol has attracted attention in the food and medical fields for its diverse pharmacological activities, including antioxidant, anti-inflammatory, cardioprotective, neuroprotective, chemopreventive, and antiaging properties.⁵⁶ However, several challenges associated with its chemical properties may limit its bioavailability, formulation, and manipulation for the development of functional foods, such as its low water-solubility, chemical instability, and quick metabolism.⁵⁹ Hence, resveratrol needs to be encapsulated within some kind of colloidal delivery system to improve its water solubility, enhance its oral bioavailability, and prolong its release time. Previous studies have used various kinds of nanocarriers to encapsulate resveratrol, including hydrophobic proteins,⁶⁰ liposomes,⁶¹ chitosan,⁶² alginate-CaCl₂ microspheres,⁶³ and cyclodextrins.⁶⁴ However, the encapsulation efficiency of resveratrol within nanocapsules increased after they were coated with chitosan (from 66.5 to 91.3%). The presence of a chitosan (CS) coating reduced the mean diameter and polydispersity index of the nanocapsules, which was attributed to their ability to inhibit particle aggregation. The chitosan coating increased the antioxidant activity and photostability of the encapsulated resveratrol, as well as improved its water-dispersibility, photostability, antioxidant activity, and prolonged its release profile.⁵⁶

The CD-MOF/CS nanocapsules were prepared using the ionic gelation.⁶⁵ Briefly, chitosan solutions were prepared by dissolving different concentrations of chitosan (1, 2, 4, or 8 mg/mL) into 1% aqueous acetic acid solutions diluted by 100% pure glacial acetic acid. The resulting solutions were then stored at 25 °C for 12 h before use to ensure hydration and dissolution. The CD cannot form a stable MOF crystal in the CS solution; therefore, a solution of γ -CD-MOF (10 mg/mL) was initially incubated for 1 h to form stable MOF crystals. Then, the chitosan solution was added dropwise into the MOF solution with constant stirring to reach a mass ratio of 1:1. This process led to the formation of CD-MOF/CS nanocapsule suspensions with final chitosan concentrations of 0.5, 1, 2, and 4 mg/mL. The nanocapsule suspensions were adjusted to a neutral pH and directly converted into a powder by freeze-drying the solution. The resveratrol-loaded nanocapsules were prepared by adding resveratrol dissolved in ethanol (4 mg/mL) to the CD-MOF solution before the CS solution. Res-CD-MOF/CS nanocapsules had a more efficient radical scavenging capacity compared to pure resveratrol (10–30% increase) (Figure 9). These results showed that the antioxidant capacity of resveratrol can be maintained and enhanced by encapsulation within CD-MOF/CS nanocapsules, potentially due to their smaller size and higher specific surface area, which provided more chances for the resveratrol to come into contact with free radicals. Wu *et al.*⁶⁶

described similar results of the radical scavenging activity of resveratrol encapsulated in CS-TPP nanoparticles, which was greater than that of free resveratrol. Resveratrol is easily degraded by light, especially UV light, which can lead to a reduction in its bioactivity and bioavailability. The free radical scavenging activity of resveratrol significantly decreased after UV irradiation; however, Res-CD-MOF/CS still remained highly reactive. These results indicated that the encapsulation of resveratrol into CD-MOF/CS nanocapsules significantly enhanced its antioxidative stability after UV exposure. Similar results were reported in studies on other types of colloidal delivery systems.⁶⁷

In vitro release studies have shown that the release of resveratrol from CD-MOFs and CD-MOF/CS nanocapsules was considerably slower, and that the maximum release was only achieved after 24 h incubation. These results indicated that the nanocapsules can be used for a prolonged release of resveratrol and that the release from CD-MOF/CS nanocapsules was greater than from the CD-MOFs, which may have been because they were less aggregated and therefore, had a more exposed surface area. Moreover, some of the resveratrol may have been solubilized within the chitosan shell surrounding the nanocapsules. The amount of resveratrol released from the CD-MOF/CS nanocapsules increased significantly after the addition of amylase, with a cumulative maximum release value of 83.9% after 24 h. This effect may have been because the digestive enzyme was able to break down the cyclodextrin and release more of the encapsulated resveratrol. Overall, the results suggest that the CD-MOF/CS nanocapsules developed in this study may be highly effective nanocarriers for hydrophobic nutraceuticals or drugs.

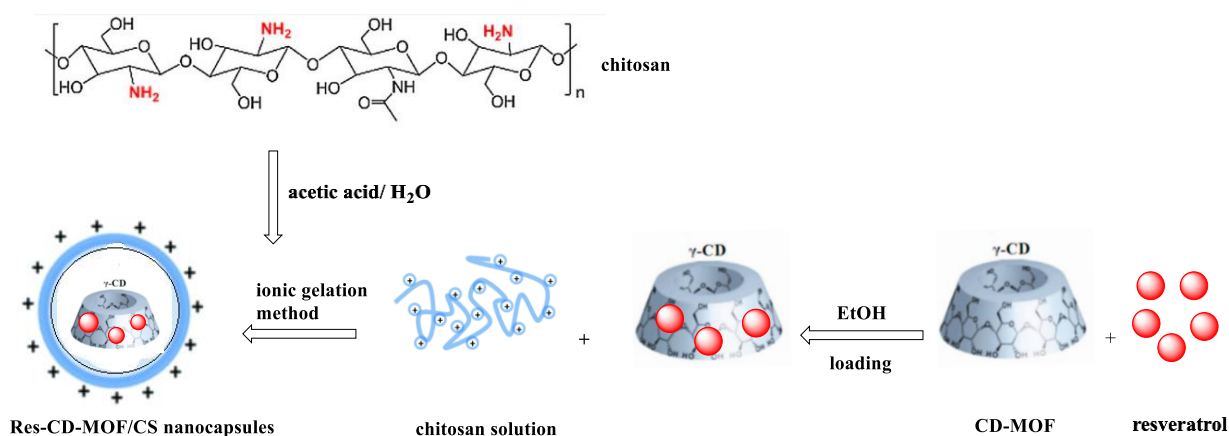


Figure 9. Schematic representation of synthesis of CD-MOF/CS for resveratrol loading

1.2.5 FER@MFM-300(SC) SYSTEM

Osorio-Toribio *et al.*⁶⁸ demonstrated that the Sc(III) MOF-type MFM-300(Sc) is stable under physiological conditions (PBS), biocompatible, and an efficient drug carrier for the long-term controlled

release of the antioxidant ferulate through human skin. MFM-300(Sc) can also preserve the antioxidant pharmacological effects of ferulate while enhancing the bio-preservation of dermal skin fibroblasts during the delivery process. Sc(III) is reactive toward proteins because it can replace Ca(II) in many biochemical events and cause negative effects in enzymatic systems and cell metabolism.⁶⁹ On the other hand, Sc(III) is successfully used as a radioactive isotope in medical applications⁷⁰ and a low concentration of Sc(III) was shown to enhance specific antibiotic overproduction and have antibacterial effects.⁷¹

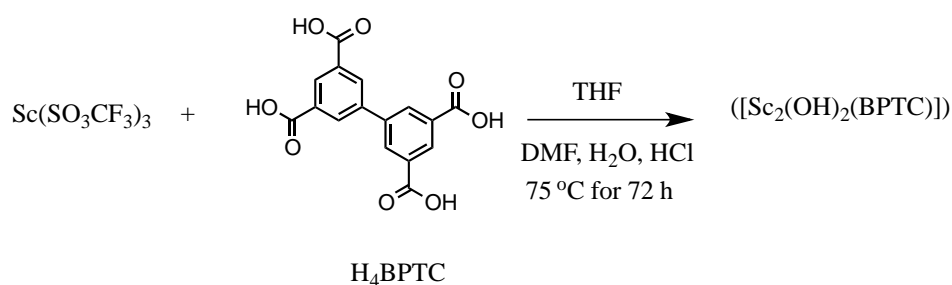
Ferulic acid (FA) is a natural antioxidant because its phenolic nucleus and unsaturated side chain allow the formation of resonance-stabilized phenoxy radicals that act as free radical scavengers.⁷² Interestingly, this molecule plays a protective role in skin structures such as collagen, fibroblasts, keratinocytes, and elastin.⁷³ Consequently, this therapeutic drug has been broadly used in skin care products as a photoprotective agent, to delay skin photoaging processes, and in the treatment of rosacea.⁷⁴ Due to the importance of FA as an active ingredient in a variety of cosmetic products, its transdermal delivery the most common route of administration. However, premature exposure to sunlight induces FA to undergo oxidation reactions that lead to the formation of quinones, dimers, and aldehydes.⁷⁵ The photodegradation of FA not only limits its shelf-life but also reduces its effectiveness before it can permeate the stratum corneum (SC), which is the most superficial layer of the epidermis, and act as skin barrier.⁷⁶ In order to avoid these limitations, FA can be encapsulated in the pores of MFM-300(Sc) to prevent photodegradation and maintain its continuous and sustained release over time and reduce frequent dosing. MFM-300(Sc) with the chemical formula $\text{Sc}_2(\text{BPTC})(\text{OH})_2$, was synthesized by mixing scandium triflate ($\text{Sc}(\text{SO}_3\text{CF}_3)_3$) (0.030 g, 0.061 mM) and biphenyl-3,3',5,5'-tetracarboxylic acid (H_4BPTC) (0.010 g, 0.030 mM) in THF (4.0 mL), DMF (3.0 mL), water (1.0 mL) and HCl (36.5%, 2 drops). The resultant mixture was stirred and heated in an oil bath at 75 °C for 72 h.

FER@MFM-300(Sc) was prepared by soaking 60 mg activated MFM-300(Sc) in an aqueous solution of ferulic acid (FA) (20 mL, 0.5 mg mL⁻¹) at pH 9. At this pH, FA is present as an anion (analogue) ferulate (FER⁻). This mixture was stirred at room temperature for 5 d and then the sample was centrifuged at for 30 min. The drug loading was estimated as 16.15 wt%, which corresponded to 0.31 mole FER⁻ per mole FER@MFM-300(Sc). The material collected was washed once with distilled water and recovered with centrifugation. Finally, the material was resuspended in 3 mL distilled water and lyophilized for 12 h at -49 °C under vacuum of 0.021 Torr (Figure 10). The incorporation of FER⁻ into MFM-300(Sc), in comparison to other well-known or commercial materials like hydrotalcites,⁷⁷ provided a long-term, controlled release through human skin.

MFM-300(Sc) also demonstrated a higher chemical stability in comparison to typical MOF drug delivery systems like MIL-100 and MIL-101.⁷⁸ The MFM-300(Sc) system improved the permeation of the drug through human skin in comparison with free FA. Such differences might be attributed to the promotion in

the absorption of FER^- inside FER@MFM-300(Sc) MOFs, potentially through transcellular or paracellular routes. In addition, there was a higher availability of the drug when it was administrated as the ion FER^- species than when it is administrated directly as a protonated species (FA). These results imply that the subsequent prolonged release of the cargo during the innocuous biodegradation of the carrier. The cytotoxicity of MFM-300(Sc) was investigated and the results demonstrated that Sc^{3+} and MFM-300(Sc) had acceptable biocompatibility for topical drug administration.

Synthesis of MFM-300(Sc)



Synthesis of FER@MFM-300(Sc)

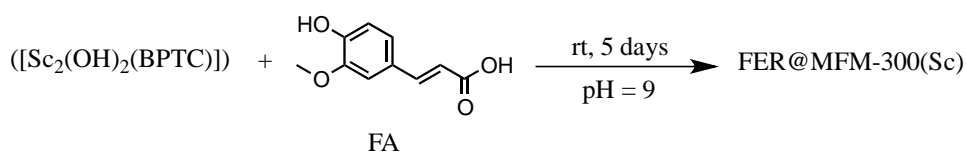


Figure 10. Synthesis of MFM-300(Sc) and FER@MFM-300(Sc)

This study revealed that the MFM-300(Sc) material improved the systemic delivery of ferulate through the controlled and sustained long-term delivery of the cargo, and reduced both the degradation of ferulate and the requirement for continuous re-application of the drug over time. These findings pave the way towards an extended use of Sc(III) -based MOFs as drug carriers.

1.2.6 QUERCETIN@ZIF-90 SYSTEM

Quercetin, which contains three aromatic rings and five-hydroxyl groups, is widely found in varieties of diet plants.⁷⁹ Many studies have demonstrated that quercetin has several clinical functions including anti-allergenic effects, osteogenic activities, and as an immune treatment.⁸⁰ Quercetin can also act as a radical scavenger or antioxidant to inhibit endogenous reactive oxygen species (ROS).⁸¹ Indeed, the radical scavenging ability of quercetin has been reported for many years,⁷⁹ but its poor absorptive properties and ambiguous metabolism are major barriers for its commercial or clinical uses. Hence, to develop a more effective use of quercetin is of great importance.

Zeolitic imidazolate frameworks (ZIFs) are a type of MOF synthesized by the strong interaction between metal ions (especially Zn and Co) and imidazole ligands.⁸² ZIFs are gaining attention in the biomedical⁸³ and biosensor⁸⁴ research fields due to their high surface area, intrinsic porosity, and biocompatibility. In addition, enzymes can be immobilized in ZIFs to increase their activity in comparison to the free enzymes.⁸⁵ It should be noted that enzymes are not susceptible to complex environments, and ZIFs could protect enzymatic functionality in more extreme conditions. It is clear that ZIFs are a reliable carrier for some bioactive molecules and could improve their stability and may potentially enhance their performance.

Xu *et al.*⁸⁶ designed the QZ nanoparticles that are synthesized by simply mixing quercetin and ZIF-90 precursors together. The QZ nanoparticles have similar characteristics to quercetin and may even be more effective than free quercetin due to the accumulation effect of ZIF.⁸⁷ The authors reported⁸⁶ a facile approach to fabricating Quercetin@ZIF-90 (QZ) nanoparticles with a narrow size distribution of about 100 nm. The nonplanar size of quercetin was about $14.294 \times 8.953 \times 4.055 \text{ \AA}$, which is a perfect size for ZIF-90 encapsulation due to its pore and window sizes of 11.2 \AA and 3.5 \AA , respectively.⁸⁸ Moreover, quercetin can chelate with Zn^{2+} , which allows for the *de novo* synthesis of QZ.⁸⁹ More specifically, quercetin and Zn^{2+} formed a complex first and then ZIF-90 crystals grew around the complex to confine quercetin in the ZIF-90 cavities. The synthesis of QZ started by mixed quercetin with 2-ICA (imidazole-2-carboxaldehyde) and $\text{Zn}(\text{OAc})_2$ in DMF (Figure 11). This study indicated that QZ had higher antioxidant and radical scavenger activity than free quercetin, suggesting this strategy provides a new method for efficient antioxidant nanoparticle synthesis with quercetin encapsulated into the ZIF-90 shell, and that the radical scavenging ability of quercetin was enhanced due to the accumulation effect of the nanoparticles under neutral conditions.

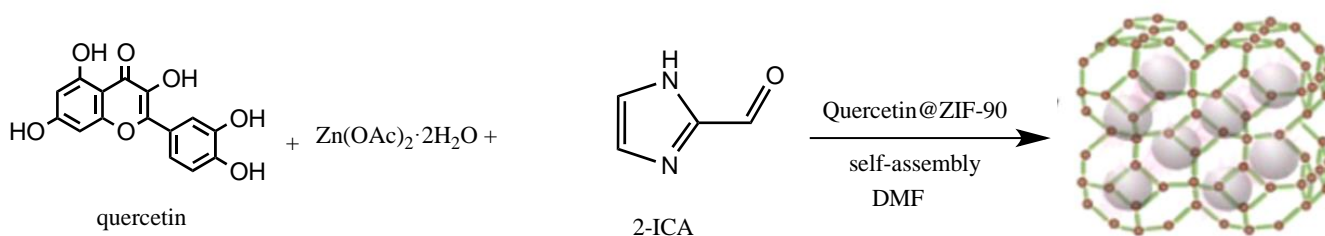


Figure 11. The synthesis of Quercetin@ZIF-90 (QZ)

Moreover, the experimental results⁸⁶ indicated that QZ was sensitive to adenosine 5'-triphosphate (ATP) and pH; thus, QZ was applied as a novel antioxidant for the determination of ATP. The 3,3',5,5'-tetramethylbenzidine (TMB) could be oxidized to a blue cation radical complex by oxidase-like BSA- MnO_2 nanosheets (MNs) at neutral pH, and QZ could sufficiently protect against MN-induced TMB

cation radical reactions, which produced no obvious color change in the MNs-TMB system after the addition of QZ. However, ATP did induce the collapse of QZ due to the interaction between ATP and Zn^{2+} , which allowed the release of quercetin from the ZIF-90 shell and the inhibition effect of the MNs was weakened, leading to the recovery of the blue oxTMB. In this manner, a novel “off-on” colorimetric method for ATP sensing was established and displayed a good linear relationship ranging from $2.0 \mu\text{mol L}^{-1}$ to $80.0 \mu\text{mol L}^{-1}$. This strategy was also capable of ATP sensing in MCF-7 cell lysates, illustrating that the method has high sensitivity and selectivity. Taken together, the study provided a novel approach for enhancing the antioxidant and radical scavenging activity of quercetin through its encapsulation in a ZIF-90 shell, and showed that the QZ-MNs-based sensing platform was capable of detecting ATP in real samples. Moreover, the unique properties of QZ such as ATP- and pH-sensitive may be important for targeted drug delivery and the investigation of quercetin metabolism.

Table 1

Group	MOF	Metal	Antioxidant Ligand	Antioxidant drug	Surface area MOF: drug	Antioxidant activity	Degradation profiles of MOFs
Antioxidant as a ligand in MOF structures	Mg(H ₂ gal) ²²	Mg (II)	Gallic acid, H ₄ gal	-	-	60 $\mu\text{g mL}^{-1}$ Mg(H ₂ gal) reduced ROS production, confirming its effective antioxidant activity.	Gallic acid is released slowly into the solution (45% after 1 d)
	MIL-155 ³⁰	Ca (II)	Gallic acid, H ₄ gal	-	-	5 mg mL^{-1} MIL-155 reduced ROS production, confirming its effective antioxidant activity.	Gallic acid is released slowly into the solution (48% after 1 d)
	MIL-156[30]	Ca (II)	Gallic acid, H ₄ gal	-	-	NA	NA
Antioxidant Encapsulated in MOFs	SC@FNPCN-333 ⁴²	Al (III)	-	antioxidant enzymes, superoxide dismutase (SOD), and catalase (CAT)	The molecular dimensions of SOD (2.8×3.5×4.2 nm ³ , 16.3 kDa) and CAT (4.9×4.4×5.6 nm ³ , kDa) indicated that these proteins could fit into the 4.0 nm and 5.5 nm cavities of FNPCN-333, respectively.	When cells were pre-treated with 75 $\mu\text{g mL}^{-1}$ SC@FNPCN-333 for 2 h, cell viability was restored, with more than 85% of cells surviving the most cytotoxic PQ treatment.	Protein leaching from the MOF was observed over 7 d in an acidic environment.
	CD-MOF/curcumin ⁵²	K	-	curcumin		NA	NA
	CD-MOF and catechins ⁵⁵	K	-	catechins	<i>Before:</i> CD-MOF (BET area and pore volume of 175 m^2g^{-1} and 0.11 cm^3g^{-1} , respectively. <i>After:</i> CD-MOF-EGCG (BET area and pore volume of 45 cm^2g^{-1} and 0.03 cm^3g^{-1} , respectively.)	As the amount of CD-MOF-EGCG increased from 1 mg to 4 mg, the antioxidant activity gradually increased from 12% to 50%.	The antioxidant activity of the free EGCG decreased significantly from 55% to 11% after 5 d. In contrast, the EGCG protected by CD-MOFs maintained its activity after 5 d. The antioxidant activity of CD-MOF-EGCG only dropped by 8% after 5 d.
	CD-MOF/chitosan-resveratrol ⁵⁶	K	-	resveratrol	The encapsulation efficiency of resveratrol increased from 66.5% to 91.3% with chitosan coating.	Compared to free resveratrol, Res-CD-MOF/CS nanocapsules exhibited a more efficient radical scavenging capacity (10–30% increase).	The amount of resveratrol released from the CD-MOF/CS nanocapsules reached a maximum value of 83.9% after 24 h.

	FER@MFM-300(Sc) ⁶⁸	Sc(III)	-	ferulate (FER ⁻)	<p><i>Before:</i> MFM-300(Sc) (BET area and pore volume of 1300 m²g⁻¹ and 0.56 cm³g⁻¹, respectively).</p> <p><i>After:</i> FER@MFM-300(Sc) (BET area and pore volume of 915 m²g⁻¹ and 0.39 cm³g⁻¹, respectively).</p>	10.40% of the ferulate (FER ⁻) permeated the skin to the systemic compartment, compared with only 5.71% of the free ferulic acid (FA) that reached the receptor compartment.	53% of the ferulate (FER ⁻) was released into the solution in approximately 4 d.
	Quercetin@ZIF-90 ⁸⁶	Zn(II)	-	quercetin	<p>The size of quercetin was about 14.294 × 8.953 × 4.055 Å, and was able to be encapsulated in ZIF-90 (11.2 and 3.5 Å) [38].</p> <p>The FTIR spectrum of QZ showed the disappearance of the characteristic peaks (–OH 3391 cm⁻¹, C=O 1664 cm⁻¹, C–O–C 1317 cm⁻¹) of free quercetin.</p>	The results demonstrated that the absorbance at 650 nm decreased after the addition of QZ or free quercetin (100.0 µg mL ⁻¹), but the ΔA after the addition of QZ was larger than quercetin alone. These observations suggested that QZ is a promising antioxidant agent that is better than free quercetin due to the accumulation effect of ZIF-90 porosity.	NA

2. CONCLUSIONS

Oxidative stress has long been linked to different diseases and decreasing this oxidative stress using different medications has been attempted. Conventional antioxidant therapies have been used for a long time but have unfortunately been minimally effective for many reasons, including their inability to cross the blood–brain barrier, which reduces their efficacy as treatment for many neurodegenerative diseases.⁹⁰ Natural and synthetic antioxidants are now outdated technologies for the management of oxidative stress-induced diseases and therefore, the development of novel and efficient delivery of therapeutic antioxidants is a pre-requisite for new therapeutic systems. New drug delivery systems have been established within the past two decades; among them, MOFs are interesting candidates due to their ability to incorporate the loading of many biologically active compounds, either within their pores or within the hybrid network itself. In addition, the active compound can be progressively released under physiological conditions through a combination of framework degradation, drug diffusion, and host–guest interactions. Unlike conventional drug carriers like micelles, liposomes, dendrimers, and mesoporous silica nanoparticles, MOFs offer a unique opportunity to modulate the incorporated drug payload and release kinetics through the engineering of their pore dimensions, which can tune the nature/strength of the adsorption sites decorating their internal pore walls, as well as of the functionalization of their external surfaces that are required for the development of formulations for the different administration routes. The active drug can be incorporated in the MOF in two main ways: (i) the active ingredient is adsorbed and entrapped inside the MOF pores, and (ii) incorporation of the active compound as either an organic or inorganic constitutive part of the MOF structure.

Loading the active molecule into the MOF structure, such as Mg(H₂gal), MIL-155 and MIL-156, has the

main advantage of avoiding multiple steps in the preparation of the loaded material, which maximizes the drug payload and the use of well-known toxicity components. In addition, the porosity of the particle is not essentially required, since the release of the active drug will happen during the degradation of the MOF. Conversely, the synthesis and structural characterization of these solids can be time-consuming due to the need to (i) optimize the crystallization conditions to reach a complete structure determination, (ii) eliminate the toxic solvents used during preparation, and (iii) control the particle size. Also, these MOFs are built from bio-compatible metal ions and may offer a synergetic effect between the cation and the linker as antioxidant (i.e., Mg and Ca as antioxidant agents).

For the drug encapsulation process of MOFs like SC@FNPCN-333, CD-MOF/curcumin, CD-MOF and catechins, CD-MOF/chitosan-resveratrol, FER@MFM-300(Sc) and Quercetin@ZIF-90 systems, the initial strategies aimed to exploit the porosity and inner chemistry of the pores to encapsulate active molecules for optimal drug loading efficiency and gradual release. These systems protect the drug from degradation under physiological conditions before they reach the targeted site and do not have toxic effects on the body. For most carrier systems, there are two basic principles that govern encapsulation. First, the concordance between the sizes of the pores and the antioxidant. Second, the chemical compatibility of the MOFs with living system. Several biocompatible MOFs have been reported that allow for the encapsulation of a broad range of large molecules while still allowing for high loading efficiency. Additionally, the easily tunable amphiphilic internal microenvironment of these MOFs, which have a polar (inorganic part) and a polar fraction (organic ligand), might be enough for the encapsulation of a large variety of hydrophobic/hydrophilic molecules. Finally, the biodegradability of the MOF is a critical parameter because once the MOF delivers its cargo to the targeted site of action and releases the encapsulated drug, it must then be eliminated from the body to avoid toxicity.

The role of the solvent during the encapsulation process must be considered to limit potential toxicity issues. Most studies reviewed here used water, methanol, and ethanol as solvents; however, the low solubility of the antioxidant as well as MOF degradability could also limit solvent use. Before investigating the parameters that control drug release from MOFs, the potential limitations from drug solubility and MOF degradability should be considered. Drug delivery can be directed by (i) MOF degradation under the physiological conditions, (ii) drug diffusion through the MOF pores, and (iii) drug–matrix and drug–solvent interactions. In addition, the conditions that affect drug release during production (i.e., composition, temperature, and stirring) must be evaluated as well as during targeted administration. Finally, due to the unique combination of the porous architecture and physicochemical properties of MOFs, they should be considered as promising drug carriers, although some of the structures are biodegradable and may be toxic, which are points that need to be addressed in *in vitro* and *in vivo* experiments, including ADME (absorption, distribution, metabolism, excretion) evaluation and efficacy

tests, before MOF formulation can be specifically adapted to each administration route.

REFERENCES

1. V. Lobo, A. Patil, A. Phatak, and N. Chandra, *Pharmacogn. Rev.*, 2010, **4**, 118.
2. P. Gupta, S. P. Authinmoolam, J. Z. Hilt, and T. D. Dziubla, *Acta Biomater.*, 2015, **27**, 194.
3. B. Halliwell, *Annu. Rev. Nutr.*, 1996, **16**, 33.
4. V. K. Koltover, *Russ. Chem. B.*, 2010, **59**, 37.
5. M. G. Simic, *Mutat. Res.*, 1988, **202**, 377.
6. N. Pellegrini, M. Serafini, B. Colombi, D. Del Rio, S. Salvatore, M. Bianchi, and F. Brighenti, *J. Nutr.*, 2003, **133**, 2812.
7. M. I. Khan and P. Giridhar, *Everyman's Science*, 2011, **46**, 214.
8. S. Medhe, P. Bansal, and M. M. Srivastava, *Appl. Nanosci.*, 2014, **4**, 153.
9. L. Li, T. B. Tg, W. Gao, W. Li, M. Fu, S.M. Niu, L. Zhao, R. R. Chen, and F. Liu, *Life Sci.*, 2005, **77**, 230.
10. A. K. Verma, *J. Pharm. Res.*, 2014, **8**, 871.
11. M. A. Anagnostopoulou, P. Kefalas, V. P. Papageorgiou, A. N. Assimopoulou, and D. Boskou, *Food Chem.*, 2006, **94**, 19.
12. Y. Liu, K. Ai, X. Ji, D. Askhatova, R. Du, L. Lu, and J. Shi, *J. Am. Chem. Soc.*, 2017, **139**, 856.
13. M. Kajita, K. Hikosaka, M. Iitsuka, A. Kanayama, N. Toshima, and Y. Miyamoto, *Free Radic. Res.*, 2007, **47**, 615.
14. S. T. Shah, W. A. Yehye, O. Saad, K. Simarani, Z. Z. Chowdhury, A. A. Alhadi, and L. A. Al-Ani, *J. Nanomater.*, 2017, **7**, 306.
15. A. Elsaesser and C. V. Howard, *Adv. Drug Deliv. Rev.*, 2012, **64**, 129.
16. A. Umemura, S. Diring, S. Furukawa, H. Uehara, T. Tsuruoka, and S. Kitagawa, *J. Am. Chem. Soc.*, 2011, **133**, 15506.
17. S. T. Meek, J. A. Greathouse, and M. D. Allendorf, *Adv. Mater.*, 2011, **23**, 249.
18. P. Horcajada, R. Gref, T. Baati, P. K. Allan, G. Maurin, P. Couvreur, G. Ferey, R. E. Morris, and C. Serre, *Chem. Rev.*, 2012, **112**, 1232.
19. S. Beg, M. Rahman, A. Jain, S. Saini, P. Midoux, C. Pichon, F. J. Ahmad, and S. Akhter, *Drug Discov. Today*, 2017, **22**, 625.
20. F. Maya, C. P. Cabello, R. M. Frizzarin, J. M. Estela, G. T. Palomino, and V. Cerda, *TrAC Trends Anal. Chem.*, 2017, **90**, 142.
21. A. U. Czaja, N. Trukhan, and U. Müller, *Chem. Soc. Rev.*, 2009, **38**, 1284.
22. L. Cooper, T. Hidalgo, M. Gorman, T. Lozano-Fernandez, R. Simon-Vasquez, C. Olivier, N. Guillou,

- C. Serre, C. Martineau, F. Tauelle, D. Damasceno-Borges, G. Maurin, A. Gonzalez-Fernandez, P. Horcajada, and T. Devic, [Chem. Commun., 2015, 51, 5848](#).
23. N. Niho, M. Shibutani, T. Tamura, K. Toyoda, C. Uneyama, N. Takahashi, and M. Hirose, [Food Chem. Toxicol., 2001, 39, 1063](#).
24. H. Deng, S. Grunder, K. E. Cordova, C. Valente, H. Furukawa, M. Hmadeh, F. Gandara, A. C. Whalley, Z. Liu, S. Asahina, H. Kazumori, M. O'Keeffe, O. Terasaki, J. F. Stoddart, and O. M. Yaghi, [Science, 2012, 336, 1118](#).
25. A. Hartwig, [Mutat. Res., 2001, 475, 113](#).
26. L. Cooper, N. Guillou, C. Martineau, E. Elkaim, F. Taulelle, C. Serre, and T. Devic, [Eur. J. Inorg. Chem., 2015, 2014, 6281](#).
27. J. Della Rocca, D. Liu, and W. Lin, [Acc. Chem. Res., 2011, 44, 957](#).
28. S. R. Miller, D. Heurtaux, T. Baati, P. Horcajada, J. M. Grenèche, and C. Serre, [Chem. Commun., 2010, 46, 4526](#).
29. S. Rojas, P. S. Wheatley, E. Quartapelle-Procopio, B. Gil, B. Marszalek, R. E. Morris, and E. Barea, [Cryst. Eng. Commun., 2013, 15, 9364](#).
30. T. Hidalgo, L. Cooper, M. Gorman, T. Loranzo-Fernandez, R. Simon-Vasquez, G. Mouchaham, J. Marrot, N. Guillou, C. Serre, P. Fertey, A. Gonzalez-Fernandez, T. Devic, and P. Horcajada, [J. Mater. Chem. B, 2017, 5, 2813](#).
31. C. C. Huang, R. S. Aronstam, D. R. Chen, and Y. W. Huang, [Toxicol. in vitro, 2010, 24, 45](#).
32. D. J. Yang, S. H. Moh, D. H. Son, S. You, A. W. Kinyua, C. M. Ko, M. Song, J. Yeo, Y. H. Choi, and K. W. Kim, [Molecules, 2016, 21](#).
33. H. J. Roh, H. J. Noh, C. S. Na, C. S. Kim, K. H. Kim, C. Y. Hong, and K. R. Lee, [Biomol. Ther., 2015, 23, 283](#).
34. T. Hintz, K. K. Matthews, and R. Di, [BioMed. Res. Int., 2015, 2015, 246](#).
35. S. Maqsood, S. Benjakul, A. Abushelaibi, and A. Alam, [Compr. Rev. Food Sci. Food Saf., 2014, 13, 1125](#).
36. I. A. Jankovic, Z. V. Saponjic, E. S. Dzunuzovic, and J. M. Nedeljkovic, [Nanoscale Res. Lett., 2010, 5, 81](#).
37. Z. Yang, K. Xiong, P. Qi, Y. Yang, Q. Tu, J. Wang, and N. Huang, [ACS Appl. Mater. Inter., 2014, 6, 2647](#).
38. B. C. Ji, W. H. Hsu, J. S. Yang, T. C. Hsia, C. C. Lu, J. H. Chiang, J. L. Yang, C. H. Lin, J. J. Lin, L. J. W. Suen, W. G. Wood, and J. G. Chung, [J. Agric. Food Chem., 2009, 57, 7596](#).
39. V. Lykourinou, Y. Chen, X. S. Wang, L. Meng, T. Hoang, L. J. Ming, R. L. Musselman, and S. Ma, [J. Am. Chem. Soc., 2011, 133, 10382](#).

40. S. L. Cao, D. M. Yue, X. H. Li, J. T. Smith, N. Li, M. H. Zong, H. Wu, Y. Z. Ma, and W. Y. Lou, [*ACS Sustain. Chem. Eng.*, 2016, **4**, 3586.](#)
41. X. Wu, J. Ge, C. Yang, M. Hou, and Z. Liu, [*Chem. Commun.*, 2015, **51**, 13408.](#)
42. X. Lian, A. Erazo-Oliveras, J. P. Pellois, and H. C. Zhou, [*Nat. Commun.*, 2017, **8**, 1.](#)
43. D. Feng, T. F. Liu, J. Su, M. Bosch, Z. Wei, W. Wan, D. Yuan, Y. P. Chen, X. Wang, and K. Wang, X. Lian, [*Nat. Commun.*, 2015, **6**, 1.](#)
44. M. Schieber and N. S. Chandel, [*Curr. Biol.*, 2014, **24**, 453.](#)
45. M. A. Hough and S. S. Hasnain, [*J. Mol. Biol.*, 1999, **287**, 579.](#)
46. K. Yonekura and S. Maki-Yonekura, [*J. Appl. Crystallogr.*, 2016, **49**, 1517.](#)
47. J. P. Luzio, P. R. Pryor, and N. A. Bright, [*Nat. Rev. Mol. Cell Biol.*, 2007, **8**, 622.](#)
48. Y. Murakami, H. Ishii, N. Takada, S. Tanaka, M. Machino, S. Ito, and S. Fujisawa, *Anticancer Res.*, 2008, **28**, 699.
49. M. Heger, R. F. van Golen, M. Broekgaarden, and M. C. Michel, [*Pharmacol. Rev.*, 2014, **66**, 222.](#)
50. H. H. Tønnesen, M. Másson, and T. Loftsson, [*Int. J. Pharm.*, 2002, **244**, 127.](#)
51. Z. Moussa, M. Hmadeh, M. G. Abiad, O. H. Dib, and D. Patra, [*Food Chem.*, 2016, **212**, 485.](#)
52. R. A. Smaldone, R. S. Forgan, H. Furukawa, J. J. Gassensmith, A. M. Slawin, O. M. Yaghi, and J. F. Stoddart, [*Angew. Chem. Int. Ed.*, 2010, **49**, 8630.](#)
53. H. C. Zhou, J. R. Long, and O. M. Yaghi, [*Chem. Rev.*, 2012, **112**, 673.](#)
54. W. Lu, Z. Wei, Z. Y. Gu, T. F. Liu, J. Park, J. Park, J. Tian, M. Zhang, Q. Zhang, T. Gentle III, and M. Bosch, [*Chem. Soc. Rev.*, 2014, **43**, 5561.](#)
55. F. Ke, M. Zhang, N. Qin, G. Zhao, J. Chu, and X. Wan, [*J. Mater. Sci.*, 2019, **54**, 10420.](#)
56. C. Qiu, D. J. McClements, Z. Jin, Y. Qin, Y. Hu, X. Xu, and J. Wang, [*Food Chem.*, 2020, **317**, 126328.](#)
57. M. C. Chen, F. L. Fi, Z. X. Liao, C. W. Hsiao, K. Sonaje, M. F. Chung, L. W. Hsu, and H. W. Sung, [*Adv. Drug Deliv. Rev.*, 2013, **65**, 865.](#)
58. L. Frémont, [*Life Sci.*, 2000, **66**, 663.](#)
59. A. Amri, J. C. Chaumeil, S. Sfar, and C. Charrueau, [*J. Control. Release*, 2012, **158**, 182.](#)
60. I. J. Joye, G. Davidov-Pardo, and D. J. McClements, [*Food Hydrocolloids.*, 2015, **49**, 127.](#)
61. M. Coimbra, B. Isacchi, L. van Bloois, J. S. Torano, A. Ket, X. Wu, F. Broere, J. M. Metselaar, C. J. Rijcken, G. Storm, and R. Bilia, [*Int. J. Pharm.*, 2011, **416**, 433.](#)
62. A. Francioso, P. Mastromarino, R. Restignoli, A. Boffi, M. d'Erme, and L. Mosca, [*J. Agric. Food Chem.*, 2014, **62**, 1520.](#)
63. A. R. Cho, Y. G. Chun, B. K. Kim, and D. J. Park, [*J. Mater. Sci.*, 2014, **49**, 4612.](#)
64. K. Kaur, S. Uppal, R. Kaur, J. Agarwal, and S. K. Mehta, [*New J. Chem.*, 2015, **39**, 8855.](#)

65. N. Ji, Y. Hong, Z. Gu, L. Cheng, Z. Li, and C. Li, [Food Funct.](#), 2018, **9**, 2902.
66. J. Wu, Y. Wang, H. Yang, X. Liu, and Z. Lu, [Carbohydr. Polym.](#), 2017, **175**, 170.
67. C. Qiu, J. Wang, H. Zhang, Y. Qin, X. Xu, and Z. Jin, [J. Agric. Food Chem.](#), 2018, **66**, 9785.
68. G. Osorio-Toribio, M. D. Velasquez-Hernandez, P. G. Mileo, J. A. Zarate, J. Aguila-Rosas, G. Leyva-Gomez, R. Sanchez-Sanchez, J. J. Magana, M. A. Perez-Diaz, I. A. Lazaro, and R. S. Forgan, [iScience](#), 2020, **23**, 101156.
69. C. Sánchez-González, C. Lopez-Chaves, L. Rivas-Garcia, P. Galindo, J. Gomez-Aracena, P. Aranda, and J. Llopis, [Sci. World J.](#), 2013, **1**.
70. K. Szkliniarz, M. Sitarz, R. Walczak, J. Jastrzebski, A. Bilewicz, J. Choinski, A. Jakubowski, A. Majkowska, A. Stolarz, A. Trzcinska, and W. Zipper, [Appl. Radiat. Isotopes](#), 2016, **118**, 182.
71. K. Kawai, G. Wang, S. Okamoto, and K. Ochi, [FEMS Microbiol. Lett.](#), 2007, **274**, 311.
72. B. Chen, S. Xiang, and G. Qian, [Acc. Chem. Res.](#), 2010, **43**, 1115.
73. Y. Z. Li, C. H. Yu, Y. T. Lin, H. L. Su, K. W. Kan, F. C. Liu, C. T. Chen, Y. T. Lin, H. F. Hsu, and Y. H. Lin, [Cosmetics](#), 2019, **6**, 17.
74. K. Zduńska, A. Dana, A. Kolodziejczak, and H. Rotsztejn, [Skin Pharmacol. Physiol.](#), 2018, **31**, 332.
75. M. Antolovich, D. R. Bedgood, A. G. Bishop, D. Jardine, P. D. Prenzler, and K. Robards, [J. Agric. Food Chem.](#), 2004, **52**, 962.
76. C. Pegoraro, S. MacNeil, and G. Battaglia, [Nanoscale](#), 2012, **4**, 1881.
77. E. Lima, J. Flores, A.S. Cruz, G. Leyva-Gómez, and E. Kröttsch, [Micropor. Mesopor. Mat.](#), 2013, **6**.
78. P. Horcajada, C. Serre, M. Vallet -Regí, M. Sebban, F. Taulelle, and G. Férey, [Angew. Chem. Int. Ed.](#), 2006, **118**, 6120.
79. J. V. Formica and W. Regelson, [Food Chem. Toxicol.](#), 1995, **33**, 1061.
80. C. A. Rice-evans, N. J. Miller, P. G. Bolwell, and P. M. Breamley, [Free Radic. Res.](#), 1995, **22**, 375.
81. L. Gibellini, M. Pinti, M. Nasi, J.P. Montagna, S. De Biasi, E. Roat, L. Bertocelli, and E. L. Cooper, A. Cossarizza, [eCAM.](#), 2011, **2011**.
82. R. Santangelo, A. Silvestrini, and C. Mancuso, [Food Chem. Toxicol.](#), 2019, **123**, 42.
83. J. Della Rocca, D. Liu, and W. Lin, [Acc. Chem. Res.](#), 2011, **44**, 957.
84. M. X. Wu and Y. W. Yang, [Adv. Mater.](#), 2017, **29**, 1606134.
85. F. Lyu, Y. Zhang, R. N. Zare, J. Ge, and Z. Liu, [Nano Lett.](#), 2014, **14**, 5761.
86. X. Xu, D. Nan, H. Yang, S. Pan, H. Liu, and X. Hu, [Sens. Actuators B Chem.](#), 2020, **304**, 127324.
87. X. Lin, G. Gao, L. Zheng, Y. Chi, and G. Chen, [Anal. Chem.](#), 2014, **86**, 1223.
88. W. Morris, C. J. Doonan, H. Furukawa, R. Banerjee, and O. M. Yaghi, [J. Am. Chem. Soc.](#), 2008, **130**, 12626.
89. G. Le Nest, O. Caille, M. Woudstra, S. Roche, F. Guerlesquin, and D. Lexa, [Inorg. Chim. Acta](#), 2004,

[357, 775.](#)

90. B. Uttara, A. V. Singh, P. Zamboni, and R. T. Mahajan, [Curr. Neuropharmacol., 2009, 7, 65.](#)
-



Shaikha Alneyadi received her PhD in organic chemistry at UAE University in 2016. In addition, she received a Master of environmental science from UAE University in 2006. She worked as a researcher at NYAD University for 1 year. From 2018 to present, Dr. Shaikha Alneyadi appointed as instructor at chemistry department in science college, UAEU. Her research interests include design and development of bioactive compounds as anti-diabetic agents and concentrate on developing new synthetic strategies to make biologically important products. Dr. Shaikha Alneyadi is the author and co-author of more than 20 papers in peer-reviewed journals, conferences, and patents.